Journal of Translational Medicine

RESEARCH

Open Access

Transcriptome changes in circulating immune cells of critical COVID-19 patients predict a specific metabolic and epigenetic imprint

Federico Virga[1,2,3,4,5*†], Daniela Taverna[4,5†], Giulio Ferrero[6,7†], Marine Leclercq[8,9], Najla El Hachem[8,9], Gerard Godoy-Tena[1,2], Cato Jacobs[10], Sonia Tarallo[11], Barbara Pardini[11], Alessio Naccarati[11], Joost Wauters[10,12], Hanne Moon Lauwers[10], Els Wauters[13,14], Pierre Close[8,9], Francesca Orso[4,5,15†] and Massimiliano Mazzone[1,2*†]

Abstract

Background The progression to critical COVID-19 arises predominantly from a dysregulated host immune response although the underlying regulatory mechanisms still remain partially elusive. This limits a prompt prediction of the disease progression, reduces the therapeutic options and restrains our understanding of "long COVID".

Methods Here, we analyzed the transcriptome of peripheral blood mononuclear cells (PBMCs) collected from COVID-19 patients experiencing different degrees of the disease (mild and critical), and control patients enrolled in the clinical trial COntAGIouS as well as independent bulk RNA-seq, single-cell RNA-seq and proteomic datasets.

Results In critical COVID-19 patients, the integrative analysis of transcriptomic data revealed an altered regulatory network involving microRNAs (miRNAs), long non-coding RNAs (lncRNAs), and coding genes that control mRNA translation-related genes, epigenetics, and metabolism. In parallel, we observed an upregulation of tRNA aminoacylation genes in critical COVID-19 patients by the analysis of either bulk or single-cell RNA-seq data from publicly available independent cohorts. Additionally, we found increased expression of coding genes enriched for the cognate amino acids (glycine, alanine, isoleucine and tyrosine), all related to protein localization, post-translational modifications, and cell metabolism in our cohort. Similar alterations in amino acid frequency were found in an independent proteomic dataset.

Conclusions Collectively, our findings indicate a broad perturbation of the gene expression landscape that characterizes the aberrant host immune response in critical COVID-19 patients and is potentially coordinated by miRNA and tRNA metabolism alterations.

†Federico Virga, Daniela Taverna and Giulio Ferrero contributed equally to this work and share first authorship.

†Massimiliano Mazzone and Francesca Orso contributed equally and share senior authorship.

*Correspondence:
Federico Virga
federico.virga@cnic.es
Massimiliano Mazzone
massimiliano.mazzone@vib-kuleuven.be

Full list of author information is available at the end of the article

Trial registration COntAGIouS, NCT04327570. Registered 26 March 2020, https://clinicaltrials.gov/ct2/show/NCT04327570.

Keywords Immune responses, SARS coronavirus, Metabolic analysis, Epigenetics, miRNA, tRNA

Introduction

Coronavirus disease 19 (COVID-19) is an infectious illness caused by severe acute respiratory syndrome coronavirus 2 (SARS-CoV-2), which led to a devastating pandemic [1]. One of the hallmarks of COVID-19 is the heterogeneity of the symptoms and, consequently, of the disease severity and final outcome [1, 2]. Before the widespread immunity from vaccination or prior infection, while the majority of infected individuals could manage to generate a prompt and effective immune response achieving viral clearance with no, or mild to moderate symptoms, others experienced critical COVID-19 disease and required hospitalization at the intensive care unit (ICU) [2]. The disease progression is largely driven by a deregulated immune system [3], both locally and systemically, causing the overwhelming inflammation that leads to tissue damage and multiple-organ failure [4]. As such, critical COVID-19 can be considered a type of viral sepsis [5]. Several reports describe many immunological features associated with disease progression such as an increased release of pro-inflammatory molecules including interleukin-6 (IL-6) and tumor necrosis factor alpha (TNFα) [3], changes in immune subset compositions [6, 7], and immune cell dysfunction such as aberrant neutrophil activation [7]. Despite this, a comprehensive understanding of the molecular and metabolic pathways that underpin the deregulated immune response is still partially elusive. This is essential since the stratification of patients at risk of progressing towards a critical disease would offer the possibility of early therapeutic intervention and the development of new treatments for disease management. Moreover, it might also help to reveal the mechanisms underlying the long-term effects of COVID-19, the so-called "long COVID", that seems related to an imprinting on the immune system [8, 9].

To study the systemic effects of SARS-CoV-2 infection on the immune compartment, we performed high-throughput sequencing of both coding and non-coding transcriptomes of peripheral blood mononuclear cells (PBMCs) isolated from COVID-19 patients experiencing different levels of disease severity and control individuals negative for SARS-CoV-2 infection.

Overall, by the use of an in-house cohort and by validating the main findings through the analysis of publicly available independent datasets (bulk and single-cell RNA-seq), we found that the critical stage of COVID-19 is characterized by profound changes in the transcriptome of circulating immune cells that possibly affect the progression of the disease. In particular, in the critical phase, we identified several deregulated microRNAs (miRNAs), such as miR-7-5p, miR-378a-3p, miR-6718-5p, miR-605-3p, miR-760, miR-7974, and miR-511-5p that could affect genes related to mRNA-translation, epigenetics, and cell metabolism. Moreover, we found an upregulation of different key enzymes involved in the transfer RNA (tRNA) aminoacylation metabolism in critical COVID-19 patients. The increase expression of the enzymes involved in tRNA metabolism correlated with a distinct amino acid-rich gene expression pattern based on the codon sequence, as well as with specific amino acid patterns in proteins upregulated in critical COVID-19 patients, as observed from an independent proteomic dataset. The most affected pathways were involved in protein localization, post-translational modifications, and cell metabolism. Finally, gene ontology analysis of the transcriptome revealed alterations in epigenetic-related genes, at least partially due to miRNA alterations, occurring during the critical course of the disease indicating a possible mechanism responsible for the "long COVID". Overall, our data indicate a cross-talk between miRNAs, genes, and tRNA metabolism that cooperate for the molecular and metabolic reprogramming of circulating immune cells during the critical stage of COVID-19.

Material and methods

Patient cohort, sampling and data collection

The research was performed as part of the COntAGIouS (COvid-19 Advanced Genetic and Immunologic Sampling; an in-depth characterization of the dynamic host immune response to coronavirus SARS-CoV-2) observational clinical trial: https://clinicaltrials.gov/ct2/show/NCT04327570. Clinical Trial Registry: https://www.clinicaltrials.gov/; clinical trial registration number: NCT04327570; date of registration: 26th March 2020. Briefly, COVID-19 patients (only adult) were recruited at the COVID-19 hospitalization wards of the tertiary care center in Leuven (Belgium) between March 2020 and February 2021. The diagnosis of COVID-19 was confirmed by positive qRT-PCR on respiratory sample and/or CT imaging compatible with SARS-CoV-2 disease. COVID-19 patients with active hematological malignancy (i) or other infectious/inflammatory conditions (ii); under calcineurin-inhibitor treatment (iii) were excluded. Additionally, all the patients that were unable or unwilling to give informed consent or the legal representatives were also excluded (iv). The control population consisted of patients with non-COVID-19 pneumonia.

Disease severity was defined as 'mild COVID-19' or 'critical COVID-19', based on the level of respiratory support at the time of sampling. The mild COVID-19 group either did not receive any respiratory support or receive oxygen *via* nasal cannula while the critical COVID-19 group received high flow oxygen support or mechanical ventilation. Following the study protocol, the blood was collected in EDTA tubes at the earliest possible timepoint after the admission. The isolation of PBMCs from EDTA tubes was performed using a lymphocyte separation medium (LSM, MP Biomedicals) following the manufacturer's standard protocol. Then, PBMC pellets were frozen in 10% dimethyl sulfoxide (DMSO, Sigma) and stored in liquid nitrogen until RNA extraction was performed. Demographic, clinical, laboratory, radiologic, treatment and outcome data from patient electronic medical records (KWS v.3.3.0) were obtained through a standardized research form in Research Electronic Data Capture Software (REDCAP, Vanderbilt University).

Extraction of RNA and library preparation for small RNA sequencing (small RNA-seq) and total RNA sequencing (RNA-seq)

RNA extraction was performed using miRNeasy Mini Kit (Qiagen) following the manufacturer's standard protocol including the DNAse step. Small RNA-seq libraries were prepared from 150 ng of total RNA extracted from PBMCs using the NEBNext Multiplex Small RNA Library Prep for Illumina kit (New England Biolabs) to convert small RNA transcripts into barcoded cDNA libraries. Each library was prepared with a unique indexed primer. Multiplex adaptor ligations, reverse transcription primer hybridization, reverse transcription reaction, and PCR amplification were performed according to the manufacturer's protocol and as described in [10]. After PCR amplification, the cDNA constructs were purified with the QIAQuick PCR Purification Kit (Qiagen), following the modifications suggested by the NEBNext® Multiplex Small RNA Library Prep for Illumina® protocol. Final libraries were quality checked on a Bioanalyzer 2100 (Agilent Technologies) using the DNA High Sensitivity Kit (Agilent Technologies) according to the manufacturer's protocol. Libraries were pooled together (in 28-plex) and further purified with a gel size selection. A final Bioanalyzer 2100 run with the High Sensitivity DNA Kit (Agilent Technologies) allowed to assess DNA libraries quality regarding size, purity, and concentration [11]. The obtained libraries were subjected to the Illumina sequencing pipeline, passing through clonal cluster generation on a single-read flow cell (75 cycles) on a NextSeq500 Sequencing System (Illumina). For total RNA-seq, 250 ~ 300 bp insert strand specific libraries were prepared using the Novogene NGS Stranded RNA Library Prep Set (PT044) after rRNA removal performed with the TruSeq Stranded Total RNA Library Prep/(Human/Mouse/Rat)/(Plant) kit. Briefly, after the rRNA removal step and fragmentation, the first strand cDNA was synthesized using random hexamer primers. Then the second strand cDNA was synthesized and dUTPs were replaced with dTTPs in the reaction buffer. The directional library was ready after end repair, A-tailing, adapter ligation, size selection, USER enzyme digestion, amplification, and purification. The libraries were checked with Qubit and real-time PCR for quantification and Bioanalyzer for size distribution detection. Quantified libraries were pooled and sequenced on Illumina platforms (NovaSeq 6000 S4 flowcell), according to effective library concentration and data amount required.

Computational and statistical analyses

Small RNA-seq and, more specifically, miRNA data analyses were performed as previously described in [12, 13]. FASTQ files from small RNA sequencing were quality-checked with FASTQC software. All reads shorter than 14 nucleotides were discarded, and the remaining reads were trimmed from the adapters using the CutAdapt software [14]. The trimmed reads were mapped against the precursor miRNA sequences downloaded from miRBase v0.22.1 with the use of BWA algorithm. Human mature miRNAs were quantified using a "knowledge-based" and a "position-based" method, as described in [12]. The identifiers of mature miRNAs quantified by the position-based approach and not annotated in miRBase were reported with the suffix "Novel". Read counts were summed in the case of miRNAs processed from different precursors but characterized by the same mature sequence. miRNA normalization and differential expression analyses (Wald test) were performed with the DESeq2 package [15]. A miRNA was defined as differentially expressed (DE) if associated with a median level greater than 15 normalized reads in at least one study group and with a Benjamini-Hochberg (BH) adjusted *p*-value lower than 0.05. The set of experimentally validated and predicted miRNA target genes was obtained using RBiomirGS v0.2.19 in default settings [16].

For total RNA-seq, raw FASTQ files were firstly quality-controlled and pre-processed with fastp in default settings [17] to remove adapter sequences and low-quality reads. Then, reads mapping on rRNA fragments were excluded using SortMeRNA v2.1b [18]. Surviving reads were aligned on Gencode v40 annotations using STAR v2.5.1b [19] in default settings and transcript levels were quantified using RSEM v1.3.0 [20]. Data normalization and differential expression analysis were then performed using tximport v1.28.0 [21] and DESeq2. A gene was defined as detected if associated with a median TPM greater than 1 in all analyzed sample groups and

considered DE if associated with a BH-adjusted *p*-value lower than 0.05. DE analyses were age and sex-adjusted.

Functional enrichment analysis of DE genes was performed with enrichR v3.2 in default settings [22] considering the libraries *GO_Biological_Process_2021*, *miRTarBase_2017*, and *COVID-19_Related_Gene_Sets.* A gene set was defined statistically enriched if associated with an adjusted *p*-value lower than 0.05. The rrvgo R package v1.12.1 [23] was applied to compute the semantic similarity among the enriched GO Biological Process terms obtained in the enrichment analysis. The analysis was performed using the Resnik method and considering a similarity threshold of 0.8. Gene-Set Enrichment Analysis (GSEA) was performed with version 4.4.0 of the Java version of the tool considering the gene set annotations from c7.immunesigdb.v2025.1.Hs. The tool was applied with default settings considering the DE genes from the critical COVID-19 vs control comparison pre-ranked based on the log2FC.

ComplexHeatmap v2.16.0 [24] was applied to generate the DE miRNAs and DE genes heatmap on Z-score-normalized miRNA/gene levels. The clustering analysis was performed using the Ward.D2 method and the Euclidean distance as clustering metric. Principal component analysis (PCA) was performed with *fviz_pca_ind* function of the *factoextra* v1.0.7 R package.

The network representation of miRNA-target interactions involving DE protein-coding or lncRNA genes was performed with Cytoscape v3.10.1 [25]. The set of protein interactions from the STRING database [26] was obtained using the stringApp available for the Cytoscape tool. The coherence of expression changes (log2FC) computed in the mild COVID-19 vs control and critical COVID-19 vs control comparisons was evaluated using the Spearman correlation method. The correlation was calculated between DE miRNA/gene log2FCs of each comparison. The progressive increase/decrease of median DE miRNA/gene levels was evaluated to estimate the candidate expression trends from control to critical COVID-19 subject samples.

Single-cell RNA-Seq data of blood samples from mild COVID-19 ($n = 8$) and critical (referred to as severe in the original article) ($n = 10$) COVID-19 patients, and from healthy controls ($n = 21$) were retrieved from the UCSC Cell Browser (https://cells.ucsc.edu/?ds=covid19-toppcell+schulte-schrepping; European Genotype-Phenotype Archive Study: EGAS00001004571), based on the provided ID in the work by Schulte-Schrepping and colleagues [27]. Dataset metadata and sparse matrix were processed using Seurat 5.1 to extract the expression levels of the genes of interest. Cluster annotations were retrieved from the publicly metadata considering the column "Cell.class_reannotated" provided by the authors.

Codon and amino acid enrichment analysis

For this analysis, downregulated genes/proteins were defined as genes/proteins with a fold change under 0.8 (Log2FC ≤= −0.32) between conditions and upregulated genes as genes with a fold change over 1.2 (Log2FC ≥= 0.26) between conditions. *P*-value was not considered. Codon enrichment analysis was performed by comparing the number of transcripts enriched in a specific codon (defined as being in the top 25% of this codon distribution in the transcriptome) in the gene set of interest to the number of enriched transcripts in the human transcriptome, using a chi-squared test as in [28]. The amino acid enrichment analysis was performed in a similar way (by comparing the amino acid distributions instead of codon one) as in [28]. The longest transcript corresponding to each gene was used in these analyses. The log2FC returned by this analysis refers to the change of the *ratio* of enriched over not enriched genes between the gene set of interest and the genome. Similarly, peptides identified through proteomic analysis were mapped to their corresponding protein identifiers and, subsequently, were matched to gene identifiers. Proteomics data were retrieved from ProteomeXChange portal (https://proteomecentral.proteomexchange.org/cgi/GetDataset?ID=PXD025265; PXD025265). For each gene, the transcript with the longest coding sequence was selected, and its codon and amino acid composition was computed. The analysis of the cumulative frequency of codons for Glycine (GLY), Threonine (THR), Tyrosine (TYR), Alanine (ALA), and Isoleucine (ILE) in the reference population (human transcriptome) and in proteins upregulated in critical patients compared to healthy controls was performed.

Results

COVID-19 progression affects the miRNome of circulating immune cells

To study the systemic effect of SARS-CoV-2 infection on circulating immune cells, we performed small RNA-seq on peripheral blood mononuclear cells (PBMCs) isolated from 19 COVID-19 patients and 8 control individuals. Specifically, we recruited COVID-19 patients, nested in the clinical study COntAGIouS (NCT04327570), that were hospitalized in ward, from hereby called mild COVID-19, or in the Intensive Care Unit (ICU), that we called critical COVID-19. Demographics and clinical characteristics are summarized in Table 1 and Table S1. Moreover, we recruited patients of the hospital tested negative for SARS-CoV-2, referred to as controls (Table 1 and Table S1), rather than healthy individuals to better distinguish COVID-19-specific pathways from those associated with pneumonia-like/inflammatory conditions.

Table 1 Demographic and clinical data of the COVID-19 patients and controls enrolled in the study

	Control (*n* = 8)	Mild COVID-19 (*n* = 6)	Critical COVID-19 (*n* = 13)	*P* value
COVID-19 disease: n (%)	0 (0)	6 (100)	13 (100)	
ICU: n (%)	0 (0)	0 (0)	13 (100)	
Age (median, ±SD)	69.5 (±7.19)	62.5 (±24.52)	68 (±12.76)	0.91
BMI (median, +SD)	26.72 (±5.02)	26.27 (±5.46)	29.07 (±5.96)	0.54
Sex				
Female: n (%)	4 (50)	4 (66.66)	3 (23.07)	0.16
Male: n (%)	4 (50)	2 (33.33)	10 (76.93)	0.16
Treatment				
Antimicrobial: n (%)	5 (62.5)	5 (83.33)	13 (100)	0.06

BMI = body mass index; ICU = intensive care unit. *P* value was assessed by Kruskal-Wallis test for age and BMI and Chi-square for sex and treatment

Small RNA-sequencing detected 863 miRNAs (median reads > 15 in at least one patients' group) (Table S2A). By age- and sex-adjusted analysis, 9 miRNAs were identified as differentially expressed (DE) (adj. $p < 0.05$; 6 up- and 3 downregulated) in COVID-19 patients (combining both mild and critical COVID-19 individuals) vs controls (Fig. 1A–D and Table S2A). More in detail, the comparison between critical COVID-19 and controls showed the major differences, with 21 DE miRNAs (14 up- and 7 downregulated), while 13 and 1 miRNAs were found differentially regulated in mild COVID-19 vs controls or mild vs critical COVID-19 patients, respectively (Fig. 1C,D and Table S2A). To further explore the miRNA expression profiles between mild and critical COVID-19 patients, we analyzed the trend of DE miRNAs considering all the DE miRNAs in at least one of the following comparisons: critical COVID-19 vs control, mild COVID-19 vs control, COVID-19 vs control and critical vs mild COVID-19. We observed a significant correlation between the altered expression of those miRNAs in critical and mild COVID-19 respect to controls (Fig. 1E). Specifically, 32 out of the 34 DE miRNAs were characterized by a coherent log2FC (Spearman rho = 0.57) (Fig. 1E), with 17 of them progressively changing in expression (10 increasing and 7 decreasing) from control to critical COVID-19 patients (Table S2A), suggesting that the critical condition displays an enhanced miRNA deregulation of around half of the DE miRNAs. Among the other small noncoding RNAs detected by small RNA-seq (549 tRNAs, 452 piRNAs, 178 snoRNAs, and 164 sncRNAs of other biotypes), 17 resulted DE between COVID-19 patients, in at least one comparison considering mild and critical COVID-19 patients together or alone vs controls (Table S2B).

COVID-19 progression alters the RNA transcripts of circulating immune cells

In the attempt to highlight the gene expression perturbations induced by COVID-19 progression, total RNA-seq was performed in a subgroup of the cohort of small RNA-seq samples (Table S1). 10,490 genes including both coding and non-coding genes such as long non-coding RNAs (lncRNAs) and pseudogenes (median Transcripts Per Million, TPM, > 1 in all study groups) were identified. Here, by age- and sex-adjusted analysis, we found 265 DE genes (adj. $p < 0.05$; 190 up- and 75 downregulated) in COVID-19 patients (including both mild and critical) vs controls (Fig. 2A–C and Table S3A). The comparison of critical COVID-19 patients vs controls revealed 502 DE genes of which 342 were upregulated and 160 downregulated (Fig. 2A–D and Table S3A). A hierarchical clustering analysis and the principal component analysis (PCA) of DE genes showed that DE genes could distinguish critical COVID-19 patients from controls (Fig. 2A,B). Among these genes, the most upregulated gene in both critical and mild COVID-19 vs controls was the key gene for the anti-viral response *IFI27* already found modulated in other datasets [29, 30] (Fig. 2C, D, Table S3A). Conversely, only 5 and 13 genes were DE in mild COVID-19 vs controls or critical vs mild COVID-19, respectively (Fig. 2A,C,D, Table S3A).

Twenty-eight out of these 502 differentially regulated genes in critical COVID-19 vs control comparison were non-coding genes. Among the 22 non-coding genes downregulated in critical COVID-19 patients were included the lncRNA *HOTAIRM1* and *GAS5* (Fig. 2E, Table S3A) that have been previously described as negative regulators of the immune response in other contexts [31, 32]. Conversely, among the 6 upregulated non-coding genes in the same comparison, we identified the lncRNA *MIR4435-2HG* (Fig. 2E, Table S3A), previously described as an inducer of intestinal inflammation [33]. Altogether, these data suggest that lncRNAs are also involved in the control of inflammatory response upon SARS-CoV-2 infection. The sequenced reads did not align to SARS-CoV-2 viral genome (data not shown), in agreement with previous publication showing no or only residual viral reads in PBMC samples of COVID-19 patients [34].

As for the miRNAs, we analyzed the trend of DE genes considering all the DE genes in at least one of the following comparisons: critical COVID-19 vs control, mild COVID-19 vs control, COVID-19 vs control and critical vs mild COVID-19 (Fig. 1E). We observed a significant correlation between the altered expression of those genes in critical and mild COVID-19 patients compared to controls (Fig. 2F). Specifically, 477 out of 511 DE genes were characterized by a coherent log2FC (Spearman rho = 0.82) (Fig. 2F), with 63 showing a progressively

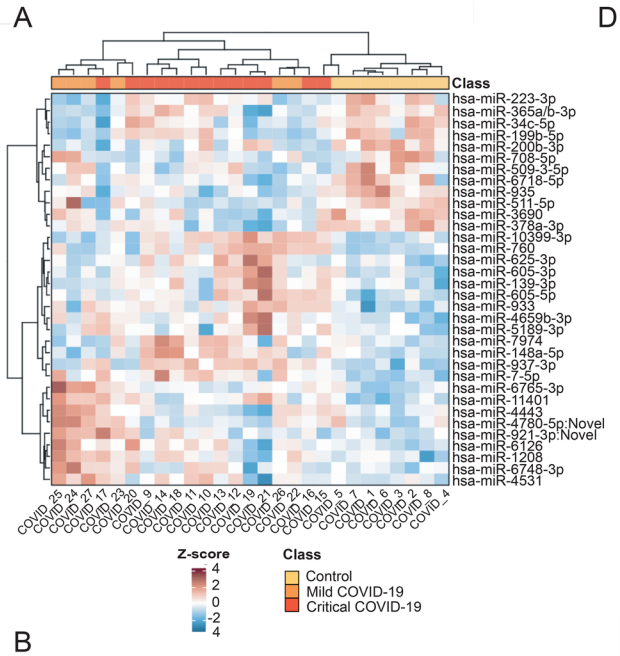

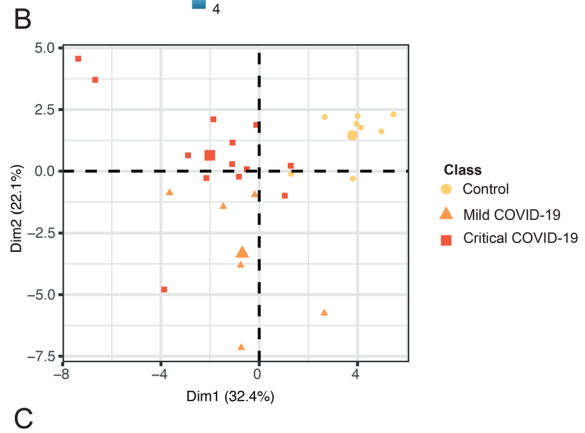

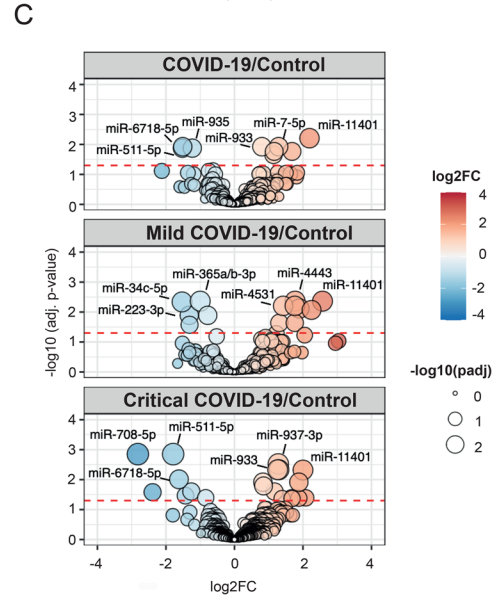

D

COVID-19/Control	
UPREGULATED	DOWNREGULATED
hsa-miR-11401	hsa-miR-511-5p
hsa-miR-4659b-3p	hsa-miR-6718-5p
hsa-miR-933	hsa-miR-935
hsa-miR-760	
hsa-miR-937-3p	
hsa-miR-7-5p	

Mild COVID-19/Control	
UPREGULATED	DOWNREGULATED
hsa-miR-11401	hsa-miR-34c-5p
hsa-miR-921-3p:Novel	hsa-miR-223-3p
hsa-miR-6748-3p	hsa-miR-199b-5p
hsa-miR-4443	hsa-miR-365a/b-3p
hsa-miR-6126	hsa-miR-200b-3p
hsa-miR-1208	
hsa-miR-4531	
hsa-miR-6765-3p	

Critical COVID-19/Control	
UPREGULATED	DOWNREGULATED
hsa-miR-7974	hsa-miR-708-5p
hsa-miR-11401	hsa-miR-509-3-5p
hsa-miR-4659b-3p	hsa-miR-511-5p
hsa-miR-5189-3p	hsa-miR-6718-5p
hsa-miR-605-3p	hsa-miR-3690
hsa-miR-605-5p	hsa-miR-935
hsa-miR-139-3p	hsa-miR-378a-3p
hsa-miR-625-3p	
hsa-miR-933	
hsa-miR-937-3p	
hsa-miR-760	
hsa-miR-148a-5p	
hsa-miR-10399-3p	
hsa-miR-7-5p	

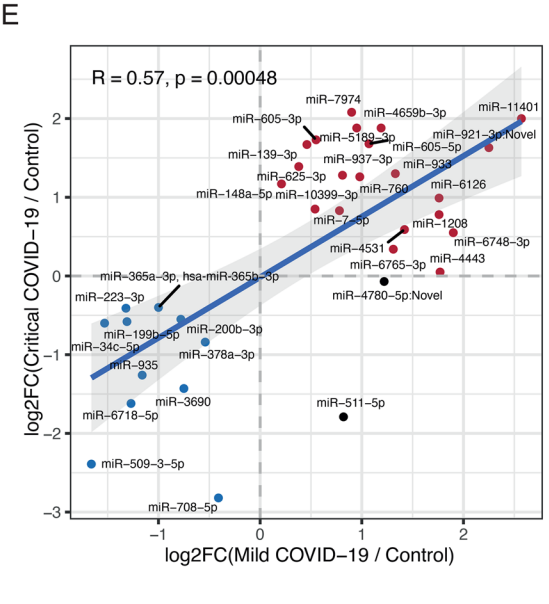

Fig. 1 (See legend on next page.)

(See figure on previous page.)

Fig. 1 COVID-19 progression affects the miRNome of circulating immune cells. (**A**) Hierarchical cluster analysis of miRNA expression profiles (Z-score normalized) represented as a heatmap depicting the differentially expressed (DE) miRNAs in PBMCs from control ($n=8$), mild COVID-19 ($n=6$), and critical COVID-19 ($n=13$) individuals. Rows indicate the identified miRNAs while columns represent the samples. The red color represents high Z-score levels while the blue color represents low Z-score levels. (**B**) Principal component analysis (PCA) of DE miRNAs in PBMC from control (in yellow; $n=8$), mild COVID-19 (in orange; $n=6$), and critical COVID-19 (in red; $n=13$) individuals. (**C**) Volcano plots depicting DE miRNAs for the indicated comparisons. Red dots represent upregulated miRNAs while blue dots represent downregulated miRNAs. Y-axis denotes -log10 adjusted *p*-value, while X-axis shows log2 fold-change (FC) values. The dashed line indicates the adjusted *p*-value threshold of 0.05. The names of the top 3 most significant up- or downregulated miRNAs were indicated on the graph. (**D**) Table displaying the DE miRNAs, ordered by decreasing log2FC, for the indicated comparisons. (**E**) Scatter plot of the relationship between the log2FC of mild and critical COVID-19 patients compared to control individuals for the DE miRNAs identified in at least one of the following comparisons: critical COVID-19 vs control, mild COVID-19 vs control, COVID-19 vs control and critical vs mild COVID-19. Spearman correlation analysis was used to calculate the correlation coefficient and *p* value. Red dots indicate miRNAs consistently upregulated in both mild and critical patients compared to controls, blue dots indicate those consistently downregulated, and black dots represent miRNAs showing inconsistent regulation between mild and critical groups. The label highlights the most significant up- and downregulated miRnas. PBMC = peripheral blood mononuclear cells

changing expression trend (55 increasing and 8 decreasing) from control to critical patients (Table S3A), further suggesting that critical conditions display an enhanced gene deregulation of a subset of genes.

Non-coding RNA-mRNA interaction analysis suggests distinct protein translation machinery, epigenetic changes, and altered metabolism in circulating immune cells of critical COVID-19 patients

Taking advantage of the data generated by both transcriptomic analyses, we investigated candidate regulatory circuits in the critical stage of the COVID-19 disease (focusing on the comparison critical COVID-19 vs controls), by exploring the DE miRNAs and their targets (validated or predicted by at least 5 prediction tools) along with experimentally supported miRNA-lncRNA interactions using lncBase v3 [35] (Table S2C–F). Moreover, using STRING [26] the validated and predicted protein-protein interactions were considered. In this way, focusing only on the genes that displayed anticorrelation with miRNAs (which suggest the canonical negative regulation of the target mediated by the miRNA [36]) or between miRNAs and lncRNAs, we obtained 5 networks (4 of them composed by two nodes) including 12 miRNAs, 8 lncRNAs, and 22 protein-coding genes (Fig. 3A-E, Table S2F). The biggest network (Fig. 3A) contained Proteasome 20S subunit alpha 3 (*PSMA3*), Ribosomal Protein S3A (*RPS3A*), Ribosomal Protein S14 (*RPS14*), Ribosomal Protein S24 (*RPS24*), Ribosomal Protein L34 (*RPL34*), NSA2 ribosome biogenesis factor (*NSA2*), Eukaryotic translation initiation factor 2 subunit gamma (*EIF2S3*), and *CD226* targeted by at least one of the following miRNAs: miR-7-5p, miR-7974, miR-605-3p, miR-760, or miR-511-5p. In addition, we identified a part of the network related to histones which included H4 clustered histone 14 (*H4C14*), a target of miR-6718-5p, and H3 clustered histone 10 (*H3C10*) targeted by miR-378a-3p that, through its cognate target *PSMA3*, connects it to the part of the network enriched with ribosome/translation related genes. Finally, miR-378a-3p and miR-3690 cooperated in the regulation of metabolic genes through the targeting of acetyl-CoA carboxylase alpha (*ACACA*) and lactate dehydrogenase A (*LDHA*). Finally, we could also appreciate that miR-7-5p was involved in interactions with both the coding (*EIF2S3*, *RPS3A*, *MARCKSL1* and *UNC119*) and non-coding (*PMS2CL*, *HOTAIRM1*, *ZFAS1*, *FMNL-DT*, *EEF1A1P5*, ENSG00000258302 and *GAS5*) elements of the transcriptome. In conclusion, our network analysis revealed several cross-talk interactions between lncRNAs, miRNAs and their targets that, overall, are possibly involved in the regulation of ribosome machinery/protein translation, epigenetics, and cell metabolism.

Circulating immune cells of critical COVID-19 patients display upregulation of a set of genes related to tRNA aminoacylation

To highlight the pathways mainly affected by the critical progression of COVID-19 and to verify the relevance of the network interactions described above at the global transcriptome level, we performed a semantic similarity analysis on the gene ontology terms enriched in the DE genes. Ten pathways were enriched in genes that were downregulated in critical COVID-19 vs control patients (Fig. 4A, Table S3B,C). Most of these genes were directly or indirectly related to protein synthesis such as "cellular macromolecular biosynthetic process", "co-translational protein targeting to the membrane" and "cytoplasmatic translation" along with "ribosome biogenesis" and "rRNA processing" (Fig. 4A) consistent with the network analysis that revealed a core of ribosome and translational-related genes negatively regulated by miRNAs (Fig. 3A). Applying the same analysis to the upregulated genes in the critical COVID-19 vs controls, 12 ontological terms were significantly enriched (Fig. 4B). Among them, there were terms related to activation of immune cells such as "antigen processing and presentation of peptide antigen via MHC class I" and "innate immune response in mucosa" (Fig. 4B). Consistent with the previous network analysis underlying a possible miRNA-epigenetic regulatory circuit (Fig. 3A), we also found enriched semantic terms related to epigenetics such as "chromatin remodeling at centromere" and "nucleosome assembly" (Fig. 4B). These data are in line with the recent observations that

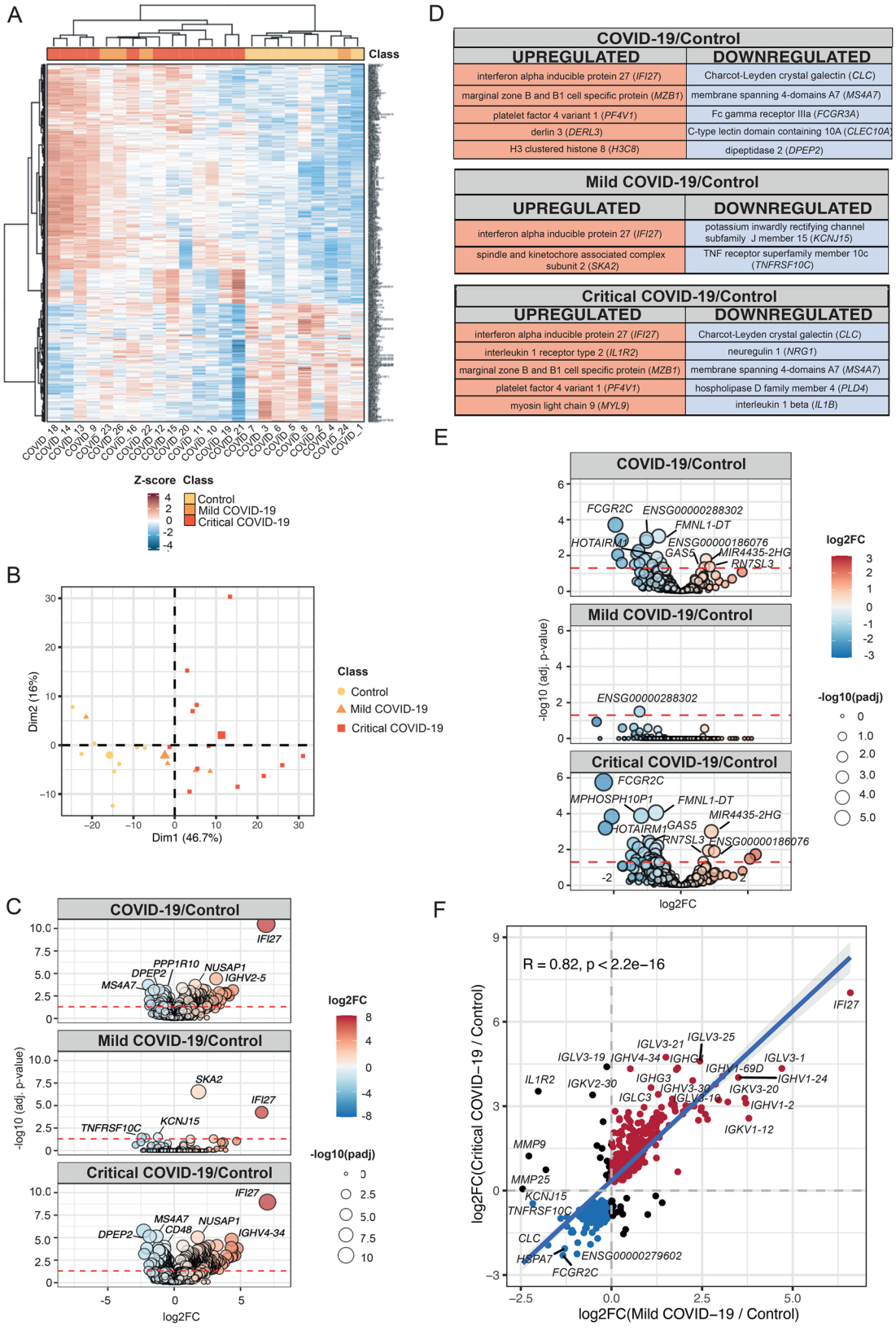

Fig. 2 (See legend on next page.)

(See figure on previous page.)

Fig. 2 COVID-19 progression alters the RNA transcripts of circulating immune cells. (**A**) Hierarchical cluster analysis of gene expression profiles (Z-score normalized) represented as a heatmap depicting the DE RNA transcripts (including coding and non-coding) in PBMC from control ($n=8$), mild COVID-19 ($n=4$) and critical COVID-19 ($n=12$) individuals. Rows indicate the identified genes while columns represent the samples. The red color represents high Z-score levels while the blue color represents low Z-score levels. (**B**) PCA of DE genes in PBMC from control in yellow ($n=8$), mild COVID-19 in orange ($n=4$), and critical COVID-19 in red ($n=12$) individuals. (**C**) Volcano plots depicting DE genes derived from (**A**), for the indicated comparisons. Red dots represent upregulated coding genes while blue dots represent downregulated coding RNAs. Y-axis denotes -log10 adjusted *p*-value, while X-axis shows log2 fold-change (FC) values. The dashed line indicates the adjusted *p*-value threshold of 0.05. The names of the top up to 3 most significant up- or downregulated coding genes are indicated on the graph. (**D**) Table displaying the top up to 5 DE protein-coding genes, ordered by decreasing log2FC, for the indicated comparisons. (**E**) Volcano plots depicting DE non-coding RNA transcripts derived from (**A**), for the indicated comparisons. Red dots represent upregulated non-coding RNAs while blue dots represent downregulated non-coding RNAs. Y-axis denotes -log10 adjusted *p*-value, while X-axis shows log2 fold-change (FC) values. The dashed line indicates the adjusted *p*-value threshold of 0.05. The names of selected up- or downregulated non-coding RNAs are indicated on the graph. (**F**) Scatter plot of the relationship between the log2FC of mild and critical COVID-19 patients compared to control individuals for DE genes. All DE genes were identified in at least one of the following comparisons: critical COVID-19 vs control, mild COVID-19 vs control, COVID-19 vs control and critical vs mild COVID-19. Spearman correlation analysis was used to calculate the correlation coefficient and *p* value. Red dots indicate genes consistently upregulated in both mild and critical patients compared to controls, blue dots indicate those consistently downregulated, and black dots represent genes showing inconsistent regulation between mild and critical groups. The label highlights the most significant up- and downregulated genes. PBMC = peripheral blood mononuclear cell

SARS-CoV-2 infections could alter the host chromatin architecture [37] and that this might be involved in the development of "long COVID" and induction of trained immunity [8, 9]. Lastly, the semantic term "tRNA aminoacylation for protein translation" was enriched too (Fig. 4B) indicating a possible influence of SARS-CoV-2 infection at the level of mRNA translation consistent with the results of the semantic similarity analysis performed on the downregulated genes (Fig. 4A). Gene-set enrichment analysis (GSEA) on DE genes in critical COVID-19 vs control, using the IMMUNESIGDB database, revealed enrichment for gene signatures associated with immune response to *Leishmania* infection and flu infection/vaccination, suggesting potential shared mechanisms of immune response (Table S3D).

Regarding tRNA aminoacylation, from the RNA-seq data, we identified 6 Aminoacyl-tRNA synthetase (ARS) genes that were upregulated in critical COVID-19 patients compared to controls: Alanyl-tRNA synthetase 1 (*AARS1*), Glutamyl-tRNA synthetase 2 mitochondrial (*EARS2*), Glycyl-tRNA Synthetase 1 (*GARS1*), Isoleucyl-tRNA Synthetase 1 (*IARS1*), Threonyl-tRNA synthetase 1 (*TARS1*), and Tyrosyl-tRNA synthetase 1 (*YARS1*) (Fig. 4C). ARSs are the key and rate-limiting enzymes for the attachment of an amino acid to its cognate transfer RNA molecule and are directly involved in mRNA translation [40].

We then checked the expression levels of these six ARS genes (Fig. 4D) in a bulk RNA-seq of PBMCs from an independent cohort of COVID-19 patients taking advantage of a publicly available dataset (GSE152418) [41]. In agreement with the data from our cohort, *AARS1, GARS1,* and *YARS1* were upregulated in the critical COVID-19 patients, referred to as "ICU" in the original article - a designation that closely matches our classification, since all critical patients in our cohort were hospitalized in the ICU. Conversely, *EARS2* was downregulated while *IARS1* and *TARS1* did not change (Fig. 4D).

Then, taking advantage of another publicly available dataset (EGAS00001004571) [27], we also analyzed the gene expression profiles at single-cell level of the indicated ARSs in circulating immune cells of COVID-19 patients from an independent cohort (Fig. 4E). Similar to the bulk RNA-seq data obtained from our cohort and from another publicly available dataset (GSE152418) [41], single-cell RNA seq analysis, using the deposited clustering and relative annotation, revealed an upregulation of *GARS1*, *IARS1, TARS1*, *YARS1* and/or *AARS1* in different circulating immune cells population at the critical stage of COVID-19 (referred to as "severe" in the original article) compared to controls (Fig. 4E). As an example, the "plasmablast" cluster showed not only an upregulation of *GARS1*, *IARS1, TARS1*, *YARS1* and/or *AARS1* (for *EARS2* the levels of expression were very low) in patients experiencing the critical stage of COVID-19 compared to controls (Fig. 4E and Fig. S1) but also an increased number of cells expressing the above-mentioned genes in the cluster (not significant for *TARS1*) (Fig. 4E and Fig. S2). Similarly, the "T/NK proliferative" and "conventional dendritic cell (cDC)" clusters showed both an increased expression levels (Fig. 4E and Fig. S1) and an increased percentage of cells expressing the *GARS1*, *IARS1, TARS1* and *YARS1* genes in patients at the critical stage of COVID-19 compared to controls (Fig. 4E and Fig. S2).

Overall, these data would suggest that different immune cells subsets, both related to innate and adaptive immunity, upregulated specific ARSs in the critical stage of COVID-19 and that could potentially contribute to the increased levels of these metabolic enzymes in the bulk RNA-seq.

Among the ARSs, EARS2 specifically catalyzes the ligation of glutamate (GLU) in the mitochondria affecting, potentially, only mitochondrial gene translation [40].

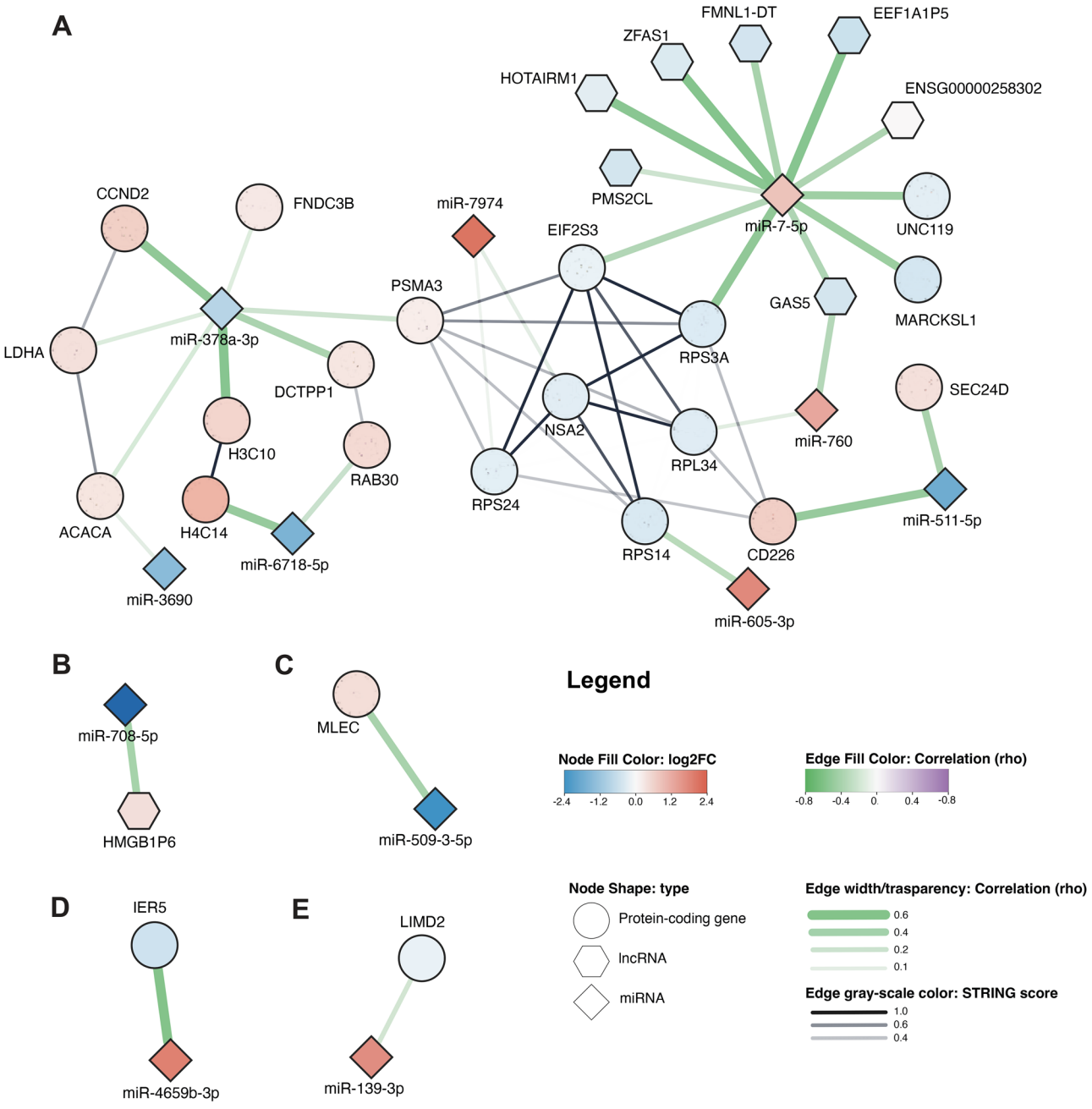

Fig. 3 Non-coding RNA-mRNA interaction analysis suggests the presence of unique protein translation machinery, epigenetic changes, and altered metabolism in the circulating immune cells of critical COVID-19 patients. (**A–E**) Interaction networks generated by connecting DE genes, miRNAs, and/or lncRNAs in critical COVID-19 vs controls. miRNA-mRNA interactions, experimentally validated or predicted by at least five prediction tools, and miRNA-lncRNA experimentally supported interactions obtained with lncBase v3 are reported and color-coded in green scale based on their Spearman correlation levels. Validated and predicted protein-protein interactions were obtained by STRING analysis and are indicated with black-grey lines. The transparency of these links is proportional to the STRING score supporting the interaction (black color = high-confidence interactions, grey = low-confidence interactions). The blue to red color scale of the nodes is proportional to the miRNA/mRNA/lncRNA expression change (blue color indicates a downregulation while red color an upregulation)

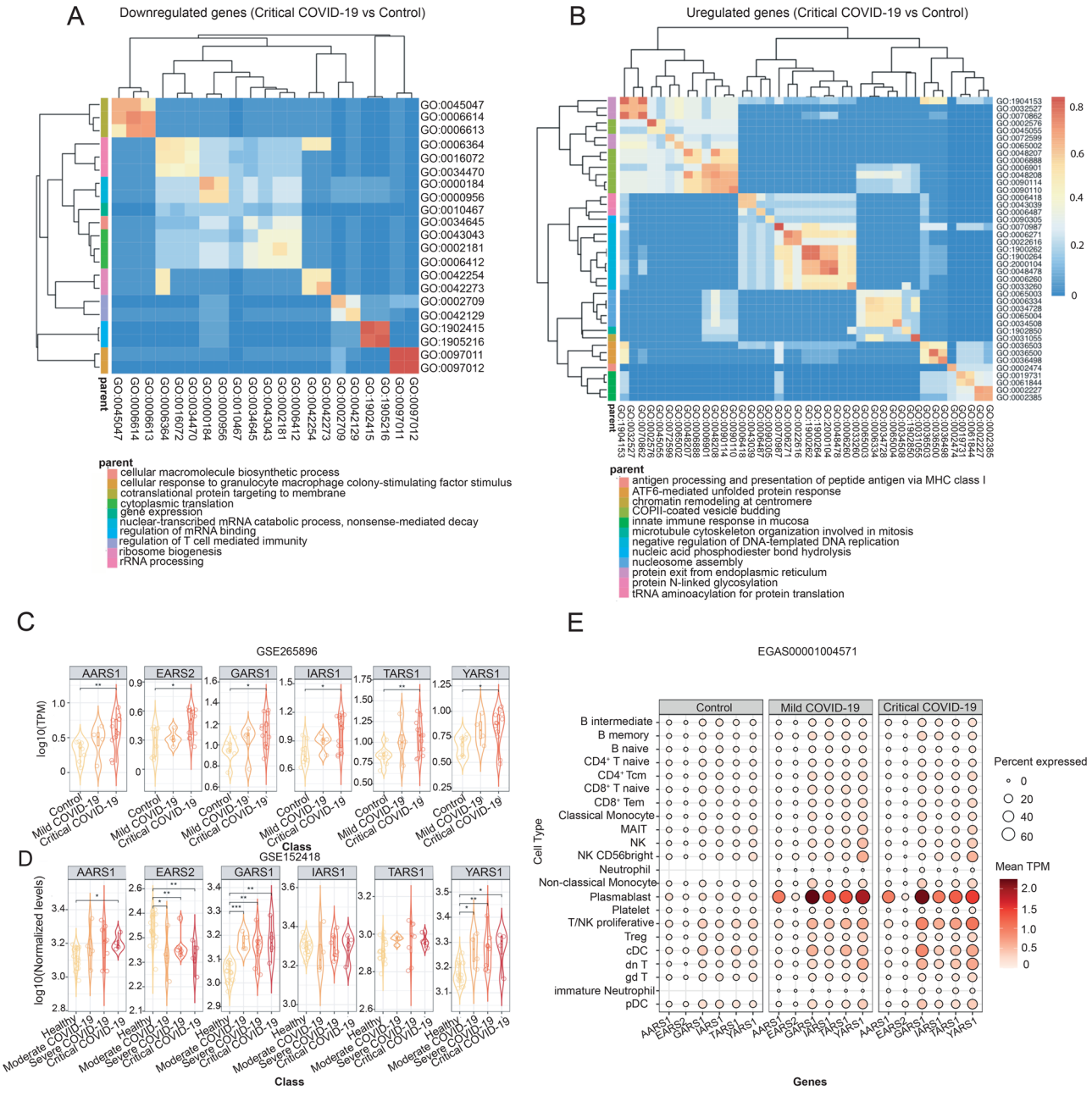

Fig. 4 Circulating immune cells from critical COVID-19 patients display upregulation of a set of genes related to tRNA aminoacylation. (**A, B**) Heatmaps reporting the semantic similarity of gene ontology (GO) biological process (BP) terms enriched in the down- (**A**) or upregulated (**B**) genes in PBMC of critical COVID-19 vs controls. The colors represent the semantic distances calculated using GOSemSim bioconductor package [38, 39] (**C, D**) Box plots reporting the expression levels of *AARS1*, *EARS2*, *GARS1*, *IARS1*, *TARS1*, and *YARS1* in our cohort: controls ($n=8$), mild COVID-19 ($n=4$), and critical COVID-19 ($n=12$) individuals, or in GSE152418: healthy ($n=17$), moderate COVID-19 ($n=4$), severe COVID-19 ($n=8$), and critical COVID-19 ($n=4$) individuals. Y axis represents the log10(TPM) (**C**) or the log10(normalized levels) (**D**). *P*-value from Wilcoxon Rank-Sum test. $^{**}p<0.01$, $^{*}p<0.05$. (**E**) Dot plot representing the levels of *AARS1*, *EARS2*, *GARS1*, *IARS1*, *TARS1*, and *YARS1* in single-cell RNA-Seq from EGAS00001004571. The dot size represents the fraction of cells expressing the genes in each specific cellular population, while the dot color represents the average expression levels (median TPM). Data are reported for patient collected and classified in control ($n=21$), mild COVID-19 ($n=8$), and critical COVID-19 ($n=10$). PBMC = peripheral blood mononuclear cells. AARS1 = Alanyl-tRNA synthetase 1, EARS2 = Glutamyl-tRNA synthetase 2, mitochondrial, GARS1 = Glycyl-tRNA synthetase 1, IARS1 = Isoleucyl-tRNA synthetase 1, TARS1 = Threonyl-tRNA synthetase 1 and YARS1 = Tyrosyl-tRNA synthetase 1 and TPM = transcript per million

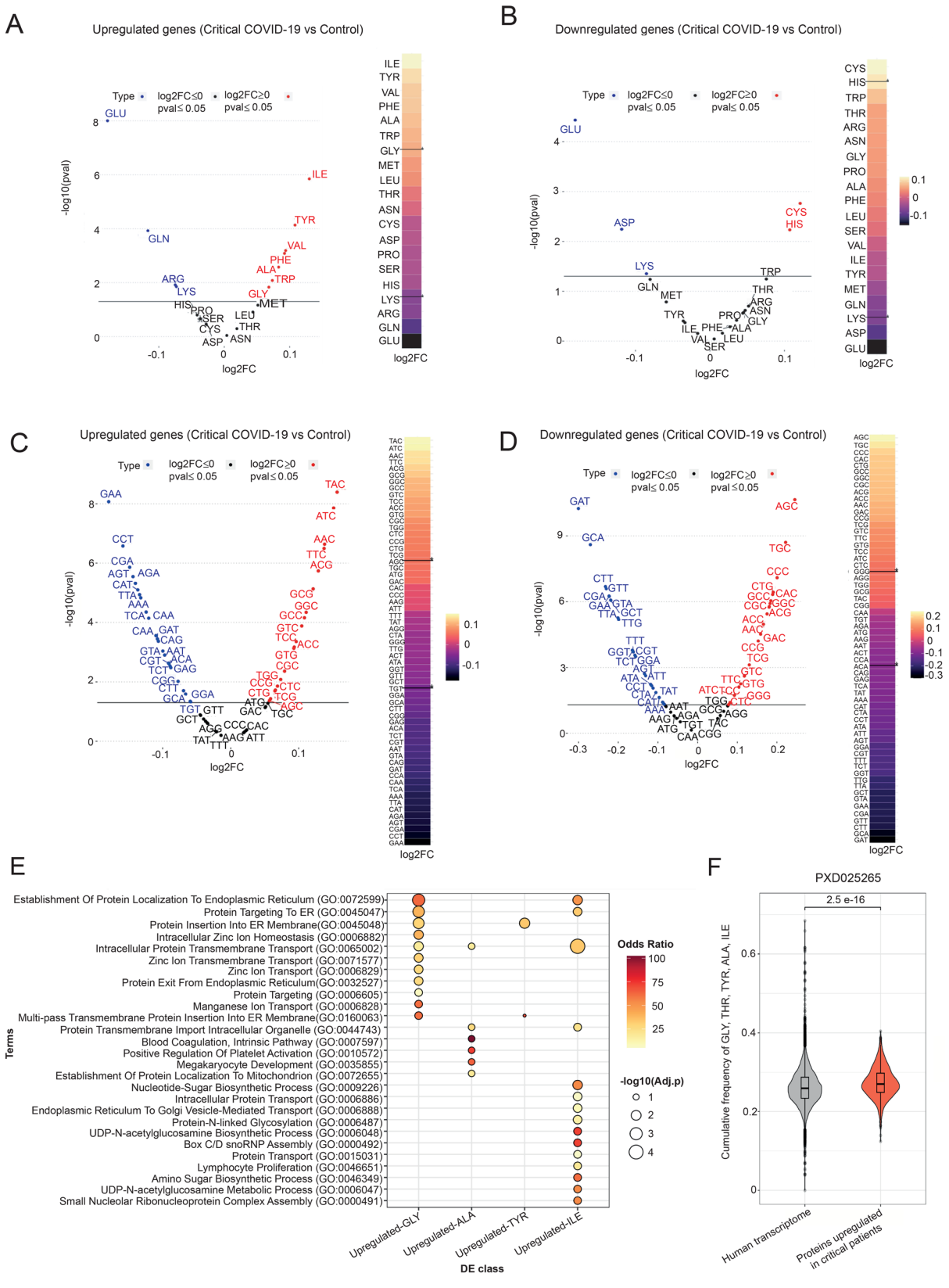

Fig. 5 (See legend on next page.)

(See figure on previous page.)

Fig. 5 Circulating immune cells from critical COVID-19 patients show alterations in amino acid usage. (**A–D**) Volcano plot depicting the enrichment analysis of the amino acids codified by the mRNA (**A**, **B**) or codons (**C**, **D**) in the transcripts of up- (**A**, **C**) and downregulated (**B**, **D**) genes from the RNA-seq of critical COVID-19 patients compared to controls. The fold change on the X-axis, reported as log2FC, indicates the ratio of enriched/not enriched genes for the individual amino acid (**A**, **B**) or codon (**C**, **D**) between the gene set and the genome. Amino acids (**A**, **B**) or codons (**C**, **D**) with negative fold change and *p*-value ≤0.05 are reported in blue; while in red are shown those with positive fold change and *p*-value ≤0.05. On the right, 1D heatmap showing the log2 FC of all the individual amino acids (**A**, **B**) or codons (**C**, **D**), black lines indicate the threshold *p*-value based on chi-squared test (≤0.05). (**E**) Up to top 15 gene ontology (GO) biological process terms enriched for the significant upregulated genes containing enriched codon for GLY, ALA, TYR, and ILE in critical COVID-19 vs controls. GO terms are ranked by analysis significance (adj. *p*-value). The dot color is proportional to the Odds ratio reflecting how enriched is the overlap of the input gene list with respect to random set of the same size. (**F**) Combined violin and box plots showing the distribution of the cumulative frequency of codons coding for of GLY, THR, TYR, ALA, and ILE codified in the reference population (human transcriptome, grey) and in the corresponding transcripts of proteins upregulated in critical patients compared to healthy controls (red). The *p*-value was obtained using Student's t-test. GLY = Glycine, THR = Threonine, TYR = Tyrosine, ALA = Alanine and ILE = Isoleucine

On the contrary, AARS1, IARS1, TARS1 and YARS1 are involved exclusively in the cytoplasmic tRNA aminoacylation of Alanine (ALA), Isoleucine (ILE), Threonine (THR), and Tyrosine (TYR), respectively. Finally, GARS1 is involved in the charging of Glycine (GLY) both in the cytoplasm and in the mitochondria [40]. These data, suggest that a different tRNA aminoacylations might be a common mechanism of COVID-19 pathogenesis.

Changes in the expression levels of tRNA aminoacylation enzymes correlate with alterations in the amino acid enrichment in circulating immune cells of critical COVID-19 patients

The differences in the expression of ARSs allowed us to speculate that immune cells of individuals experiencing a critical stage of COVID-19 might reprogram their gene expression by increasing the mRNA transcription and translation of genes enriched in ALA, ILE, THR, TYR, GLY (while only protein synthesized in the mitochondria enriched in GLU should be positively affected by the upregulation of *EARS2*). To test this hypothesis, we performed an amino acid enrichment analysis on all the up- and downregulated genes in the critical COVID-19 vs control comparison (genes with a fold change above 1.2 or under 0.8, respectively). As expected, among the seven amino acids most enriched in the upregulated genes there were GLY, ALA, TYR, and ILE, while the enrichment of THR in the upregulated genes was not significant (Fig. 5A and Table S3E). Notably, TARS1 regulation was not conserved in the other bulk RNA-seq dataset GSE152418 (Fig. 4D). When looking at the downregulated genes in critical COVID-19, the enrichment for these amino acids was lost (Fig. 5B), suggesting that this could be a mechanism to increase the expression of a specific set of disease-related genes. Interestingly, we could also identify an enrichment of specific codons both in up- and downregulated genes. In particular, 19 and 21 codons were more enriched, while 24 and 23 were less enriched in up- and downregulated genes, respectively (Fig. 5C,D).

To understand if ARS regulation could be a potential mechanism to regulate specific pathways, we performed a gene ontology analysis on the genes that both displayed an enrichment for the specific amino acids GLY, ALA, TYR or ILE and that were upregulated (fold change over 1.2) in the critical COVID-19 patients compared to controls (Fig. 5E and Table S3F). In this analysis, the gene ontology terms "Establishment of protein localization to endoplasmic reticulum", "Intracellular protein transmembrane transport", "Protein insertion into ER Membrane", "Protein transmembrane import into intracellular organelle" were enriched in at least one of the four amino acids: GLY, ALA, TYR, or ILE (Fig. 5E). In addition, glycine-enriched upregulated genes were also involved in metal ion transport and metabolism ("Zinc ion transport", "Intracellular Zinc Ion Homeostasis", and "Manganese ion transport"); while isoleucine-enriched-genes in different metabolic pathways including "Protein N-linked Glycosylation", "UDP-N-acetylglucosamine biosynthetic and metabolic process", and "amino sugar biosynthetic process" (Fig. 5E). Overall, these data would suggest an upregulation, dependent on the amino acid content encoded by the transcript, of genes involved in protein localization, post-translational modifications, and cell metabolism in the critical stage of COVID-19.

Finally, using a publicly available proteomic dataset of PBMCs isolated from COVID-19 patients (PXD025265) [42] we found that, in agreement with our predictions based on the upregulation of *AARS1*, *GARS1*, *IARS1*, *TARS1*, and *YARS1* in our cohort (Fig. 4C), there is an increased cumulative frequency of the distribution of codons for ALA, GLY, ILE, THR and TYR in the corresponding transcripts of proteins upregulated in critical patients compared to healthy controls, using the human transcriptome as reference (Fig. 5F). Overall, these findings further suggest an altered amino acid preference in mRNA translation in circulating immune cells of COVID-19 patients, that might affect disease outcomes.

Discussion

A better understanding of the host pathogen interactions is essential for the further development of strategies to manage COVID-19 and its long-term effects. Despite the big efforts to characterize the pathophysiology of

SARS-CoV-2 infection, the reasons why the clinical presentation of COVID-19 involves such a broad range of symptoms and disease trajectories are still partially elusive.

Here, to gain insights into the regulatory mechanisms triggered at the systemic level in response to SARS-CoV-2 infection, we combined the sequencing of both miRNAs and genes expressed in PBMCs isolated from control patients, negative for SARS-CoV-2, and COVID-19 patients experiencing different degrees of the disease nested in the clinical study COntAGIouS (NCT04327570). Our transcriptome data revealed a complex alteration of the gene expression landscape, including miRNAs, lncRNAs, epigenetic genes and tRNA synthetase enzymes, that overall contribute to the critical stage of the COVID-19 disease (Fig. 6). One of the limitations of the study is the size of the cohort and the unequal number of individuals across groups, particularly in the case of mild COVID-19 patients. Despite this, our findings are consistent with and complementary to existing literature. Importantly, key findings have been validated using independent datasets.

The PCA analysis of the transcriptomes from COVID-19 patients and controls suggests that mild COVID-19 cases occupy an intermediate transcriptional state between SARS-CoV-2–negative controls and critical COVID-19 patients. Furthermore, the fold changes and expression trends of DE genes and miRNAs across conditions indicate that critical COVID-19 patients exhibit a more pronounced deregulation—characterized by either further up- or downregulation of a specific subset of transcripts. These observations allow us to speculate that SARS-CoV-2 infection induces a virus-specific perturbation of the immune response, which, if exacerbated, may contribute to progression toward the critical stage of the disease.

Aligned with our data on critical COVID-19 patients, miRNome analysis in whole blood samples from an Indian cohort of COVID-19 patients revealed an upregulation of miR-4659b-3p, miR-605, and miR-760 in severe or dead patients compared to healthy controls [43]. Conversely, a similar study identified a set of miRNAs altered in whole blood from severe patients such as miR-15b-5p, miR-486-3p and, –5p that we found unchanged in our cohort [44]. Moreover, many efforts have been made to identify miRNAs as possible biomarkers in blood-derived biological fluids. Interestingly, among the top upregulated miRNAs in critical COVID-19 patients, we found miR-937-3p that has been previously found upregulated in plasma of symptomatic patients and even more in severe patients [45]. Our result is consistent with the current literature and would suggest that miR-937-3p found in plasma can derive from immune/stromal cells as previously showed for other miRNAs [46, 47]. Concerning miR-378a-3p, there are conflicting results among studies: in swab specimens of severe COVID-19 vs control individual, miR-378a-3p levels were found downregulated [48], while they were upregulated in the serum samples of severe [49] or mild [50] COVID-19 patients compared to controls. Critical COVID-19 patients often evolve to viral sepsis and miR-7-5p is overexpressed in the circulating exosomes upon sepsis onset [51], therefore this increase can be very likely linked to the septic process.

Based on the generated transcriptomic data and the application of different bioinformatic methods to isolate reliable molecular interactions, we built a comprehensive network of miRNAs, lncRNAs and genes. This network analysis revealed that miR-378a-3p and miR-6718-5p might be involved in the epigenetic regulation of circulating immune cells by targeting histone genes, consistent with the idea that a subgroup of miRNAs, called epi-miRNAs, can take part to epigenetic regulatory circuitries [52]. A possible epigenetic regulation triggered by SARS-CoV-2 infection in our cohort was further suggested by the enrichment of semantic terms including nucleosome assembly and chromatin remodeling at the centromere. These data are in line with single cell RNA sequencing data from PBMCs of COVID-19 patients [53]. Moreover, single-cell ATAC-seq profiles of PBMCs in convalescing COVID-19 patients compared to those in healthy donors also revealed chromatin remodeling in the immune cell compartment [9]. In particular, this study shows that SARS-CoV-2 elicits a memory response not only in the adaptive immune system but also in the innate immune system (in monocytes), a process named trained immunity. Consistently, a more recent publication reported that these epigenetic changes can persist up to 1 year after severe COVID-19, strongly suggesting that this mechanism might contribute to the development of "long COVID" [8]. The "long COVID" is a multisystemic condition with insufficient clinical therapeutic options characterized by more than 200 possible symptoms (such as fatigue, dyspnea and cognitive impairment) and an estimated incidence of at least 10% of the infected people [54]. Overall, our data suggest that immune cells are trained by SARS-CoV-2 infection and that this imprinting might be relevant in the development of "long COVID". Epigenetic changes and epi-miRNAs should be investigated as therapeutic targets in the future. In this line, several therapeutic strategies targeting miRNAs are already being explored and, in infectious diseases, miR-122, a liver-specific miRNA that regulates lipid metabolism and hepatitis C virus (HCV) replication, has been successfully targeted using the locked nucleic acid (LNA) inhibitor miravirsen [55]. Miravirsen demonstrated antiviral efficacy and good safety profiles in clinical trials, providing a proof-of-concept that miRNA-based therapies can be effective in humans [55].

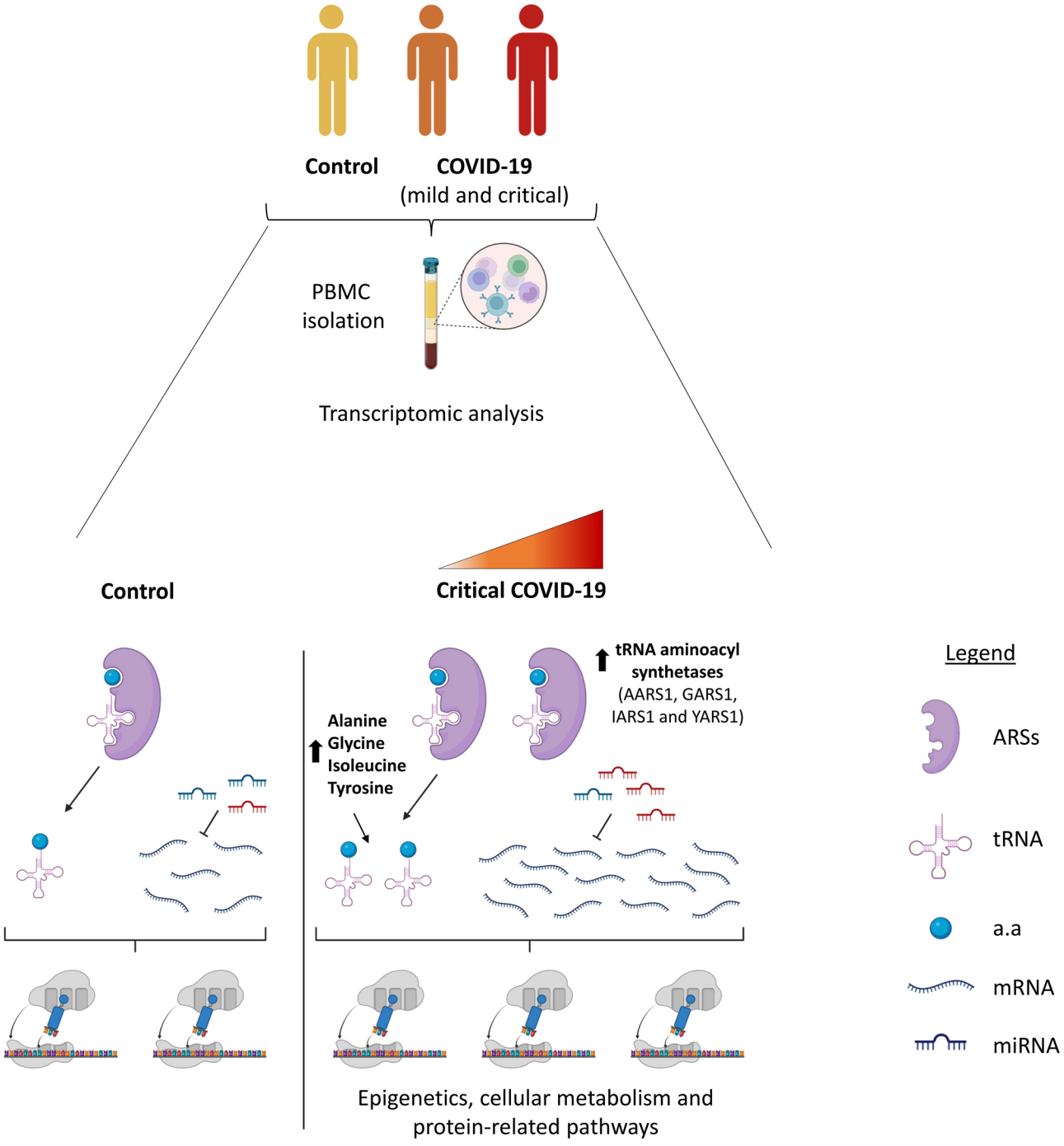

Fig. 6 Schematic overview of the study workflow and main findings. Transcriptomic analysis was performed on RNA-seq data obtained from PBMCs isolated from control and COVID-19 patients (mild and critical). PBMCs from critical COVID-19 patients show alterations in miRNAs and genes involved in tRNA metabolism (specifically at least for aminoacyl-tRNA Synthetases AARS1, GARS1, IARS1 and YARS). Additionally, expression of coding genes enriched for the cognate amino acids (at least glycine, alanine, isoleucine and tyrosine) were upregulated in critical cases. Overall, critical patients showed dysregulation in pathways related to epigenetics, cellular metabolism, and protein-related pathways compare to control individuals. The Figure was created with Biorender.com. AARS1=Alanyl-tRNA synthetase 1, GARS1=Glycyl-tRNA Synthetase 1, IARS1=Isoleucyl-tRNA Synthetase 1, and YARS1= Tyrosyl-tRNA synthetase 1

Besides the network, the analysis on the transcriptome also revealed a deregulation of key enzymes in the tRNA aminoacylation metabolism. ARSs play a major role in protein synthesis since they are involved in the ligation of the appropriate amino acid to its cognate tRNA. While in the past ARSs were considered housekeeping genes, accumulated evidence shows that alterations in tRNA metabolism contribute to pathological processes such as cancer and neurological disorders [56–58], as shown for other metabolic pathways [59, 60]. Here, our transcriptomic analysis reveals an upregulation of *GARS1*, *AARS1*, *IARS1*, *TARS1* and *YARS1*, similarly to what found in an independent cohort of COVID-19 patients in comparable disease stages [41] or at single-cell resolution in an independent cohort [27], suggesting that alterations in tRNA metabolism might be a possible mechanism occurring during SARS-CoV-2 pathogenesis. Consistently, the upregulation of these ARSs correlates with the increased expression of mRNA transcripts enriched in codons for GLY, ALA, ILE, or TYR in our cohort and with an increased enrichment of GLY, ALA, ILE, THR or TYR amino acids in proteins upregulated in critical patients compared to healthy individuals in an independent proteomic dataset. Notably, blood of COVID-19 patients displays strong alterations in the amino acid profile [61]. For example, a study reports that low levels of ALA, GLY and TYR, among others, inversely correlate with IL-6 plasma levels (used in the study as a readout of COVID-19 severity) showing a similar trend for Tryptophan (TRP) which is converted in kynurenine by the immune system and contributes to COVID-19 progression [62, 63]. Another study not only confirmed the reduced circulating levels of ALA and GLY, but, by performing a metabolite set enrichment analysis in the plasma, also showed that amino acid related pathways (including tRNA charging) are predominantly affected upon SARS-CoV-2 infection [64]. These data let us to speculate that modulation of mRNA translation by ARSs, in different subsets of circulating immune cells, can contribute to the well-documented alterations of amino acids in the blood of COVID-19 patients.

Recently the canonical role of ARSs in the immune response has been explored highlighting the importance of tRNA aminoacylation for both cellular and humoral responses. In cancer, a subset of B cells highly expressing leucine-tRNA-synthetase-2 (LARS2) displays an enhanced mitochondrial protein biosynthesis affecting B cell metabolism leading to a TGF-β-mediated immunosuppression phenotype that supports cancer progression [65]. Consistently, the sticky (*sti*) mutation in AARS has been shown to affect B lymphocytes by reducing their cell numbers while enhancing antibody production [66]. AARS mutation affects also T cell receptor (TCR) signaling in T cells [66]. In the context of viral infection, the genetic knockdown of the leucyl-tRNA synthase (LARS), in macrophage-like THP1 cell line dampens the induction of inflammatory genes attenuating the response to Hepatitis E virus (HEV) [67]. Similarly, our data could suggest that a set of amino acid-rich genes, in our case involved in protein localization, post-translational modifications, and cell metabolism, could be specifically modulated by their cognate cytoplasmatic ARSs upon SARS-CoV-2 infection. Most of these pathways were previously related to COVID-19 progression such as glycosylation which fits with the reported higher glycan biosynthesis/glycation in inflammatory monocytes, $CD4^+$ T cells, and plasma cells [68] or localization of protein to the endoplasmic reticulum, found enriched in B cells of COVID-19 patients [53]. Moreover, Zinc metabolism, another pathway enriched in our cohort of critical COVID-19, is essential for immune activation during infection and Zinc supplementation has demonstrated positive effects and potential therapeutic benefits in the treatment of COVID-19 [69].

Conclusion

In conclusion, by mining the transcriptome of PBMCs from individuals with critical COVID-19, this study identified miRNAs and pathways associated with COVID-19 severity and defined alteration in tRNA aminoacylation, overall impacting on protein modifications, cell metabolism, and epigenetic. These elements of the transcriptome could be utilized for stratifying individuals developing the critical disease stage in addition to providing future avenues for expanding the understanding of the immunobiology of COVID-19 as well as possible targets for therapeutic intervention. Further longitudinal studies, as well as the analysis of larger and independent cohorts, are required to determine the prognostic value of these molecular players and their potential involvement in the development of "long COVID" symptoms.

Abbreviations

AARS1	Alanyl-tRNA synthetase 1
ALA	Alanine
ARS	Aminoacyl-tRNA synthetase
BMI	Body mass index
cDC	Conventional dendritic cell
COVID-19	Coronavirus disease 2019
DE	Differentially expressed
EARS2	Glutamyl-tRNA synthetase 2 mitochondrial
GARS1	Glycyl-tRNA Synthetase 1
GLY	Glycine
HEV	Hepatitis E virus
IARS1	Isoleucyl-tRNA Synthetase 1
ICU	Intensive care unit
IL-6	Interleukin-6
ILE	Isoleucine
LARS2	Leucine-tRNA-synthetase-2
LNA	Locked nucleic acid
lncRNAs	Long non-coding RNAs
miRNAs	MicroRNAs
PBMCs	Peripheral blood mononuclear cells

PCA	Principal component analysis
SARS-CoV-2	Severe acute respiratory syndrome coronavirus 2
TARS1	Threonyl-tRNA synthetase 1
TCR	T cell receptor
THR	Threonine
TNFα	Tumor necrosis factor alpha
tRNA	Transfer RNA
TRP	Tryptophan
TYR	Tyrosine
YARS1	Tyrosyl-tRNA synthetase 1

Supplementary Information

The online version contains supplementary material available at https://doi.org/10.1186/s12967-025-07665-y.

Supplementary Material 1

Supplementary Material 2

Supplementary Material 3

Supplementary Material 4

Acknowledgements
The authors would thank Lotte Vanheer for her help to upload the raw data on EGA.

Author contributions
Conceptualization, M.M., F.V., F.O., D.T. and G.F.; methodology and investigation, F.V., D.T., G.O., N.EH., M.L., G. GT., S.T. and B.P.; formal analysis, G.F., F.V., D.T., N.EH., M.L, B.P., resources, C.J., J.W., H.M.L. and E. W.; writing – original draft, F.V., F.O., M.M and G.F.; writing – review & editing, D.T. M.L., J.C., S.T., B.P., A.N., J.W., H.M.L., E.W. and P.C.; supervision, F.V, M.M and F.O.; funding acquisition: M.M., D.T. and F.O.

Funding
This work was supported by FISR 2020, Fondo Integrativo Speciale per la Ricerca (ref. FISR2020IP_02024) and UNITO-Compagnia di San Paolo, Bando ex-post 2020 grants. FV was partially supported by Juan de la Cierva Investigadores fellowship (JDC2022-048924-I) funded by MCIN/AEI/10.13039/501100011033 and Next GenerationEU/PRTR. FO was partially funded by the Italian Ministry of University and Research (MUR) Program "Department of Excellence 2023-2027", AGING Project - Department of Translational Medicine, Università del Piemonte Orientale. We also thank Novogene for the RNA sequencing. MM and PC were supported by the Fonds Wetenschappelijk Onderzoek – Excellence of Science grant (FWO-EOS Grant 40007564).

Data availability
Raw and processed small RNA-Seq (EGAD50000001406) and total RNA-Seq data (EGAD50000001405) are available at the European Genome-phenome Archive (EGA) portal.

Declarations

Ethics approval and consent to participate
All study procedures were performed in accordance with the Declaration of Helsinki and approved by the Ethics Committee of the University Hospitals Leuven (Belgium, S63881). Informed consent was obtained from all individuals or their legal guardians. The research was performed as part of the observational clinical COntAGIouS (COvid-19 Advanced Genetic and Immunologic Sampling) registered under the number NCT04327570 on ClinicalTrials.gov.

Consent for publication
All authors have agreed to publish this manuscript.

Competing interests
The authors declare no competing interests.

Author details
[1]Laboratory of Tumor Inflammation and Angiogenesis, Center for Cancer Biology, VIB, Leuven, Belgium
[2]Department of Oncology, Laboratory of Tumor Inflammation and Angiogenesis, Center for Cancer Biology, KU Leuven, Leuven, Belgium
[3]Spanish National Centre for Cardiovascular Research Carlos III, Madrid 28029, Spain
[4]Department of Molecular Biotechnology and Health Sciences, University of Torino, Torino, Italy
[5]Molecular Biotechnology Center, University of Torino, Torino, Italy
[6]Department of Clinical and Biological Sciences, University of Torino, Turin, Italy
[7]Department of Computer Science, University of Torino, Turin, Italy
[8]Cancer Signaling, GIGA Stem Cells, Liège University, Liège, Belgium
[9]WELBIO Department, WEL Research Institute, Wavre, Belgium
[10]Medical Intensive Care Unit, Department of General Internal Medicine, University Hospitals Leuven, Leuven, Belgium
[11]Italian Institute for Genomic Medicine, Turin, Italy
[12]Department of Microbiology, Immunology, and Transplantation, Laboratory of Clinical Infectious and Inflammatory Disorders, KU Leuven, Leuven, Belgium
[13]Department of Respiratory Diseases, University Hospitals Leuven, Leuven, Belgium
[14]Department of Chronic Diseases and Metabolism, Laboratory of Respiratory Diseases and Thoracic Surgery (BREATHE), KU Leuven, Leuven, Belgium
[15]Department of Translational Medicine (DIMET), University of Piemonte Orientale, Novara, Italy

Received: 10 September 2025 / Accepted: 29 December 2025
Published online: 22 January 2026

References

1. Meyerowitz EA, Scott J, Richterman A, Male V, Cevik M. Clinical course and management of COVID-19 in the era of widespread population immunity. Nat Rev Microbiol. 2024;22(2):75–88.
2. Lamers MM, Haagmans BL. SARS-CoV-2 pathogenesis. Nat Rev Microbiol. 2022;20(5):270–84.
3. Del Valle DM, Kim-Schulze S, Huang HH, Beckmann ND, Nirenberg S, Wang B, et al. An inflammatory cytokine signature predicts COVID-19 severity and survival. Nat Med. 2020;26(10):1636–43.
4. Purbey PK, Roy K, Gupta S, Paul MK. Mechanistic insight into the protective and pathogenic immune-responses against SARS-CoV-2. Mol Immunol. 2023;156(2022):111–26.
5. Zhang Y, Han J. Rethinking sepsis after a two-year battle with COVID-19. Cell Mol Immunol. 2022;19(11):1317–18.
6. Lucas C, Wong P, Klein J, Castro TBR, Silva J, Sundaram M, et al. Longitudinal analyses reveal immunological misfiring in severe COVID-19. Nature. 2020;584(7821):463–69.
7. Vanderbeke L, Van Mol P, Van Herck Y, De Smet F, Humblet-Baron S, Martinod K, et al. Monocyte-driven atypical cytokine storm and aberrant neutrophil activation as key mediators of COVID-19 disease severity. Nat Commun. 2021;12(1):1–15.
8. Cheong JG, Ravishankar A, Sharma S, Parkhurst CN, Grassmann SA, Wingert CK, et al. Epigenetic memory of coronavirus infection in innate immune cells and their progenitors. Cell. 2023;186(18):3882–902.e24.
9. You M, Chen L, Zhang D, Zhao P, Chen Z, Qin EQ, et al. Single-cell epigenomic landscape of peripheral immune cells reveals establishment of trained immunity in individuals convalescing from COVID-19. Nat Cell Biol. 2021;23(6):620–30.
10. Pardini B, Ferrero G, Tarallo S, Gallo G, Francavilla A, Licheri N, et al. A fecal microRNA signature by small RNA sequencing accurately distinguishes Colorectal Cancers: results from a multicenter study. Gastroenterology. 2023;165(3):582–99.e8.
11. Francavilla A, Gagliardi A, Piaggeschi G, Tarallo S, Cordero F, Pensa RG, et al. Faecal miRNA profiles associated with age, sex, BMI, and lifestyle habits in healthy individuals. Sci Rep. 2021;11(1):1–15.
12. Tarallo S, Ferrero G, Gallo G, Francavilla A, Clerico G, Realis Luc A, et al. Altered fecal small RNA profiles in colorectal cancer reflect gut microbiome composition in stool samples. mSystems. 2019;4(5):1–16.

13. Ferrero G, Cordero F, Tarallo S, Arigoni M, Riccardo F, Gallo G, et al. Small non-coding RNA profiling in human biofluids and surrogate tissues from healthy individuals: description of the diverse and most represented species. Oncotarget. 2018;9(3):3097–111.
14. Martin M. Cutadapt removes adapter sequences from high-throughput sequencing reads. EMBnetjournal. 2011;17(1). Gener Seq Data Anal.
15. Love MI, Huber W, Anders S. Moderated estimation of fold change and dispersion for RNA-seq data with DESeq2. Genome Biol. 2014;15(12):1–21.
16. Zhang J, Storey KB. RBiomirGS: an all-in-one miRNA gene set analysis solution featuring target mRNA mapping and expression profile integration. PeerJ. 2018;2018(1):1–17.
17. Chen S, Zhou Y, Chen Y, Gu J. Fastp: an ultra-fast all-in-one FASTQ preprocessor. Bioinformatics. 2018;34(17):i884–90.
18. Noé L, Touzet H. SortMeRNA: Fast and accurate filtering of ribosomal RNAs in metatranscriptomic data, Bioinform. 2012;28(24):3211–7.
19. Dobin A, Davis CA, Schlesinger F, Drenkow J, Zaleski C, Jha S, et al. STAR: ultrafast universal RNA-seq aligner. Bioinformatics. 2013;29(1):15–21.
20. Li B, Dewey CN. RSEM: accurate transcript quantification from RNA-Seq data with or without a reference genome. BMC Bioinf. 2011;12(1):323.
21. Soneson C, Love MI, Robinson MD. Differential analyses for RNA-seq: transcript-level estimates improve gene-level inferences. F1000Res. 2016;4:1–23.
22. Xie Z, Bailey A, Kuleshov MV, Clarke DJB, Evangelista JE, Jenkins SL, et al. Gene set knowledge discovery with Enrichr. Curr Protoc. 2021;1(3):1–84.
23. Sayols S. Rrvgo: a bioconductor package for interpreting lists of gene ontology terms. MicroPubl Biol. 2023;2023.
24. Gu Z. Complex heatmap visualization. iMeta. 2022;1(3):1–15.
25. Shannon P, Markiel A, Ozier O, Baliga NS, Wang JT, Ramage D, et al. Cytoscape: a software environment for integrated models of biomolecular interaction networks. Genome Res. 2003;13(11):2498–504.
26. Szklarczyk D, Kirsch R, Koutrouli M, Nastou K, Mehryary F, Hachilif R, et al. The STRING database in 2023: protein-protein association networks and functional enrichment analyses for any sequenced genome of interest. Nucleic Acids Res. 2023;51(1 D):D638–46.
27. Schulte-Schrepping J, Reusch N, Paclik D, Baßler K, Schlickeiser S, Zhang B, et al. Severe COVID-19 is marked by a dysregulated myeloid cell compartment. Cell. 2020;182(6):1419–40.e23.
28. El-Hachem N, Leclercq M, Susaeta Ruiz M, Vanleyssem R, Shostak K, Körner PR, et al. Valine aminoacyl-tRNA synthetase promotes therapy resistance in melanoma. Nat Cell Biol. 2024;26(7):1154–64.
29. Shojaei M, Shamshirian A, Monkman J, Grice L, Tran M, Tan CW, et al. IFI27 transcription is an early predictor for COVID-19 outcomes, a multi-cohort observational study. Front Immunol. 2023;13.
30. Wang Y, Li J, Zhang L, Sun HX, Zhang Z, Xu J, et al. Plasma cell-free RNA characteristics in COVID-19 patients. Genome Res. 2022;32(2):228–41.
31. Thakuri BKC, Zhang J, Zhao J, Nguyen LN, Nguyen LNT, Khanal S, et al. LncRNA HOTAIRM1 promotes MDSC expansion and suppressive functions through the HOXA1-miR124 axis during HCV infection. Sci Rep. 2020;10(1):1–12.
32. Zeng Z, Lan Y, Chen Y, Zuo F, Gong Y, Luo G, et al. LncRNA GAS5 suppresses inflammatory responses by inhibiting HMGB1 release via miR-155-5p/SIRT1 axis in sepsis. Eur J Pharmacol. 2023;942:175520.
33. Cao L, Tan Q, Zhu R, Ye L, Shi G, Yuan Z. LncRNA MIR4435-2HG suppression regulates macrophage M1/M2 polarization and reduces intestinal inflammation in mice with ulcerative colitis. Cytokine. 2023;170:156338.
34. Moustafa A, Khalel RS, Aziz RK. Traces of SARS-CoV-2 RNA in peripheral blood cells of patients with COVID-19. Omics J Integr Biol. 2021;25(8):475–83.
35. Karagkouni D, Paraskevopoulou MD, Tastsoglou S, Skoufos G, Karavangeli A, Pierros V, et al. DIANA-LncBase v3: indexing experimentally supported miRNA targets on non-coding transcripts. Nucleic Acids Res. 2020;48(D1):D101–10.
36. Virga F, Quirico L, Cucinelli S, Mazzone M, Taverna D, Orso F. MicroRNA-mediated metabolic shaping of the tumor microenvironment. Cancers. 2021;13(1):127.
37. Wang R, Lee JH, Kim J, Xiong F, Al Hasani L, Shi Y, et al. SARS-CoV-2 restructures host chromatin architecture. Nat Microbiol. 2023;8(4):679–94.
38. Yu G, Li F, Qin Y, Bo X, Wu Y, Wang S. GOSemSim: an R package for measuring semantic similarity among GO terms and gene products. Bioinformatics. 2010;26(7):976–78.
39. Yu G. Gene ontology semantic similarity analysis using GOSemSim. In: Kidder BL, editor. Stem cell transcriptional networks: methods and protocols. New York, NY: Springer US; 2020. p. 207–15.
40. Nie A, Sun B, Fu Z, Yu D. Roles of aminoacyl-tRNA synthetases in immune regulation and immune diseases. Cell Death Dis. 2019;10(12).
41. Arunachalam PS, Wimmers F, Mok CKP, Perera RAPM, Scott M, Hagan T, et al. Systems biological assessment of immunity to mild versus severe COVID-19 infection in humans. Science. 2020;369(6508):1210–20.
42. Carapito R, Li R, Helms J, Carapito C, Gujja S, Rolli V, et al. Identification of driver genes for critical forms of COVID-19 in a deeply phenotyped young patient cohort. Sci Transl Med. 2022;14(628):eabj7521.
43. Srivastava S, Garg I, Singh Y, Meena R, Ghosh N, Kumari B, et al. Evaluation of altered miRNA expression pattern to predict COVID-19 severity. Heliyon. 2023;9(2):e13388.
44. Tang H, Gao Y, Li Z, Miao Y, Huang Z, Liu X, et al. The noncoding and coding transcriptional landscape of the peripheral immune response in patients with COVID-19. Clin Transl Med. 2020;10(6):1–18.
45. Fernández-Pato A, Virseda-Berdices A, Resino S, Ryan P, Martínez-González O, Pérez-García F, et al. Plasma miRNA profile at COVID-19 onset predicts severity status and mortality. Emerg Microbes Infect. 2022;11:676–88.
46. Virga F, Cappellesso F, Stijlemans B, Henze AT, Trotta R, van Audenaerde J, et al. Macrophage miR-210 induction and metabolic reprogramming in response to pathogen interaction boost life-threatening inflammation. Sci Adv. 2021;7(19).
47. Orso F, Virga F, Dettori D, Dalmasso A, Paradzik M, Savino A, et al. Stroma-derived miR-214 coordinates tumor dissemination. J Exp Clin Cancer Res. 2023;42(1):20.
48. Garnier N, Pollet K, Fourcot M, Caplan M, Marot G, Goutay J, et al. Altered microRNA expression in severe COVID-19: potential prognostic and pathophysiological role. Clin Transl Med. 2022;12(6):1–6.
49. Giannella A, Riccetti S, Sinigaglia A, Piubelli C, Razzaboni E, Di Battista P, et al. Circulating microRNA signatures associated with disease severity and outcome in COVID-19 patients. Front Immunol. 2022;13:1–21.
50. Nicoletti AS, Visacri MB, Ronda CRS, Vasconcelos PENS, Quintanilha JCF, Souza RN, et al. Differentially expressed plasmatic microRNAs in Brazilian patients with Coronavirus disease 2019 (COVID-19): preliminary results. Mol Biol Rep. 2022;49(7):6931–43.
51. Deng J, Li YQ, Liu Y, Li Q, Hu Y, Xu JQ, et al. Exosomes derived from plasma of septic patients inhibit apoptosis of T lymphocytes by down-regulating bad via hsa-miR-7-5p. Biochem Biophys Res Commun. 2019;513(4):958–66.
52. Reale E, Taverna D, Cantini L, Martignetti L, Osella M, De Pittà C, et al. Investigating the epi-miRNome: identification of epi-miRNAs using transfection experiments. Epigenomics. 2019;11(14):1581–99.
53. Zhu L, Yang P, Zhao Y, Zhuang Z, Wang Z, Song R, et al. Single-cell sequencing of peripheral mononuclear cells reveals distinct immune response landscapes of COVID-19 and influenza patients. Immunity. 2020;53(3):685–96.e3.
54. Davis HE, McCorkell L, Vogel JM, Topol EJ. Author correction: Long COVID: major findings, mechanisms and recommendations (Nature Reviews Microbiology, (2023), 21, 3, (133-146), 10.1038/s41579-022-00846-2). Nat Rev Microbiol. 2023;21(6):408.
55. Janssen HLA, Reesink HW, Lawitz EJ, Zeuzem S, Rodriguez-Torres M, Patel K, et al. Treatment of HCV infection by targeting microRNA. N Engl J Med. 2013;368(18):1685–94.
56. Orellana EA, Siegal E, Gregory RI. tRNA dysregulation and disease. Nat Rev Genet. 2022;23(11):651–64.
57. Rapino F, Delaunay S, Rambow F, Zhou Z, Tharun L, De Tullio P, et al. Author correction: Codon-specific translation reprogramming promotes resistance to targeted therapy (Nature, (2018), 558, 7711, (605-609), 10.1038/s41586-018-0243-7). Nature. 2021;599(7886):E14.
58. Jeong SJ, Kim JH, Lim BJ, Yoon I, Song JA, Moon HS, et al. Inhibition of muc1 biosynthesis via threonyl-trna synthetase suppresses pancreatic cancer cell migration. Exp Mol Med. 2018;50(1):e424–13.
59. Virga F, Ehling M, Mazzone M. Blood vessel proximity shapes cancer cell metabolism. Cell Metab. 2019;30(1):16–18.
60. Cappellesso F, Mazzone M, Virga F. Acid affairs in anti-tumour immunity. Cancer Cell Int. 2024;24(1):354.
61. Masoodi M, Peschka M, Schmiedel S, Haddad M, Frye M, Maas C, et al. Disturbed lipid and amino acid metabolisms in COVID-19 patients. J Mol Med. 2022;100(4):555–68.
62. Badawy AAB. The kynurenine pathway of tryptophan metabolism: a neglected therapeutic target of COVID-19 pathophysiology and immunotherapy. Biosci Rep. 2023;43(8):1–22.
63. Almulla AF, Supasitthumrong T, Tunvirachaisakul C, Algon AAA, Al-Hakeim HK, Maes M. The tryptophan catabolite or kynurenine pathway in COVID-19 and critical COVID-19: a systematic review and meta-analysis. BMC Infect Dis. 2022;22(1):615.

64. Krishnan S, Nordqvist H, Ambikan AT, Gupta S, Sperk M, Svensson-Akusjärvi S, et al. Metabolic perturbation associated with COVID-19 disease severity and SARS-CoV-2 replication. Mol Cell Proteomics. 2021;20:0–14.
65. Wang Z, Lu Z, Lin S, Xia J, Zhong Z, Xie Z, et al. Leucine-tRNA-synthase-2-expressing B cells contribute to colorectal cancer immunoevasion. Immunity. 2022;55(6):1067–81.e8.
66. Shim JA, Jo Y, Hwang H, Lee SE, Ha D, Lee JH, et al. Defects in aminoacyl-tRNA synthetase cause partial B and T cell immunodeficiency. Cell Mol Life Sci. 2022;79(2):87.
67. Li Y, Zhang R, Wang Y, Li P, Li Y, Janssen HLA, et al. Hepatitis E virus infection remodels the mature tRNAome in macrophages to orchestrate NLRP3 inflammasome response. Proc Natl Acad Sci USA. 2023;120(25):e2304445120.
68. Lee JW, Su Y, Baloni P, Chen D, Pavlovitch-Bedzyk AJ, Yuan D, et al. Integrated analysis of plasma and single immune cells uncovers metabolic changes in individuals with COVID-19. Nat Biotechnol. 2022;40(1):110–20.
69. Jin D, Zhong L, Lu H. The nutritional roles of zinc for immune system and COVID-19 patients. 2024;19:1–10.

Publisher's Note